Single-Crystal and Polycrystalline Morphology of the Thiophene-Based Semiconductor α-Hexathienyl (α-6T)

Andrew J. Lovinger,* D. D. Davis, A. Dodabalapur, H. E. Katz, and L. Torsi

Bell Laboratories, Lucent Technologies, Murray Hill, New Jersey 07974

Received January 25, 1996; Revised Manuscript Received April 18, 1996[⊗]

ABSTRACT: We have conducted a detailed electron-microscopic investigation of the structure and morphology of α-hexathienyl (α-6T), a hexameric homologue of polythiophene that shows great promise as a thin-film-transistor material. In ordinary films for device applications prepared by vacuum sublimation, α-6T crystals are very small (<100 nm), irregular, and preferentially oriented parallel to the substrate. By crystallization from the melt, very broad (tens of micrometers) and thin lamellar crystals are obtained, with their molecules perpendicular to the lamellar surfaces. Single-crystal electron-diffraction patterns from a variety of zones allow resolution of the main-chain repeat at 2.38 nm, recording of over 30 orders of intramolecular reflections, discrimination among the four proposed unit cells, and determination of the preferred crystal-growth direction (which corresponds to the unique *b*-axis of the monoclinic cell). In addition, we have shown that the lamellae undergo splaying and warping about an axis corresponding to their growth direction, as well as very extensive fractures perpendicular to that axis. These fractures are explained based upon poor interdigitation of the flat extended-chain molecules between their densely packed (020) planes. By introducing such extensive internal disruptions to the lattice, these cleavage planes are expected to have severe negative implications on single-crystal transistor characteristics.

Introduction

The last five years have seen an enormous increase in interest in organic and polymeric semiconducting materials. While these are certainly not expected to replace silicon, they offer appealing advantages in terms of processability (e.g., through low-temperature evaporation or solution-casting), fabrication over large areas in a potentially continuous process, mechanical and thermal compatibility with flexible plastic substrates, etc. Polythiophene[1−3] and poly(phenylenevinylene)[4,5] have been the polymeric semiconductors most widely studied to date. However, there are clear advantages to maximizing crystallinity where electronic transport is concerned, and the minimization of amorphous regions and grain boundaries is highly desirable. The above polymers yield amorphous to semicrystalline films in their solid states, as is inherent in chain defects introduced during polymerization, intermolecular entanglements, etc. For this reason, a number of groups, most notably and extensively Garnier *et al.*[6−8] starting in the late 1980s, have been exploring the properties of low-molecular-weight analogues of these polymers of thiophene and have provided detailed and seminal information on their semiconducting properties and applications. The most promising of these thiophenes is the hexamer, α-hexathienyl (α-6T). Through careful and controlled synthesis and purification, we were able to obtain[9,10] a melting point as high as 312 °C, a mobility of up to 0.03 cm^2/V s, and a source-drain on/off current ratio of $>10^6$. An extensive review of these materials has recently been published.[11]

The molecules of α-6T have been found to adopt an essentially planar all-trans conformation and to pack in a herringbone array.[12−15] A number of different structures have been proposed over time, all monoclinic. The earliest unit cell was by Servet and co-workers,[12] who proposed a $P2_1/c$ symmetry with chains parallel to the long axis of a cell having dimensions $a = 0.598$ nm, $b = 0.780$ nm, $c = 5.028$ nm, and $\beta = 111.3°$. A subsequent detailed Rietvelt analysis from polycrystalline specimens[13] found a unit cell with $a = 4.538$ nm, $b = 0.786$ nm, $c = 0.603$ nm, $\beta = 99.0°$, and space group $P2_1/a$. A major characteristic of this cell is that the molecular chains are inclined to its axes. A more recent study by Horowitz et al.[14] originated from a single-crystal X-ray analysis and found very similar dimensions and chain orientation to those proposed by Porzio et al.,[13] but in a cell that is almost metrically orthorhombic ($a = 4.471$ nm, $b = 0.785$ nm, $c = 0.602$ nm, $\beta = 90.76°$, space group $P2_1/n$). In addition, from macroscopic single crystals grown within a temperature gradient,[16] we recently determined the structure of a high-temperature form of α-6T, which we found to have the smallest unit cell reported so far, i.e., $a = 0.914$ nm, $b = 0.568$ nm, $c = 2.067$ nm, $\beta = 98°$, and space group $P2_1/a$.[15] The molecules are once again planar and highly inclined to their cell axes.

Despite this high activity regarding structural determination, there has been very little work on the morphology of α-6T. We have performed an electron-microscopic investigation of films used for transistor applications[17] and found a polycrystalline morphology of thin lamellae (ca. 100−200 nm long and 15−30 nm thick). A remarkable feature of these was that their constituent molecules had a preferred orientation nearly normal to their substrates. This orientation is important in conjunction with the two-dimensional mechanism of transport found for this semiconductor.[9] Here we extend our morphological study to single crystals as well as to bulk polycrystalline samples.

Experimental Section

α-Hexathienyl was synthesized and purified as described earlier.[10,18] Single crystals were grown for examination by transmission electron microscopy and diffraction in a variety of ways. Vapor growth was effected by slow sublimation under high vacuum (10^{-5}−10^{-6} Torr) in an evaporator directly onto carbon-coated electron-microscope grids. For growth from the melt, ultrathin films (≤200 nm thick) were cast from dilute solution in mesitylene onto freshly cleaved mica under dry

[⊗] Abstract published in *Advance ACS Abstracts,* June 1, 1996.

S0024-9297(96)00111-8 CCC: $12.00

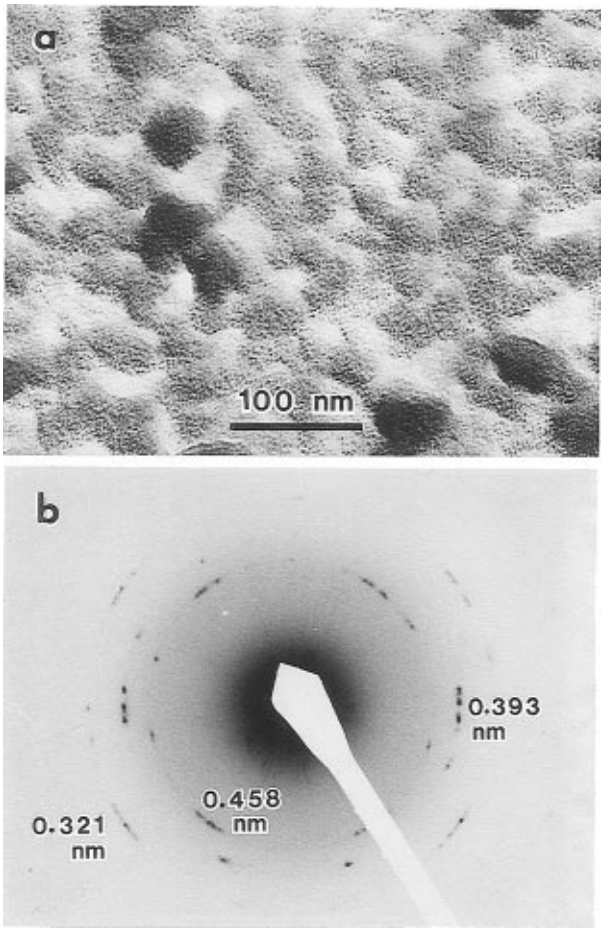

Figure 1. (a) Transmission electron micrograph and (b) selected-area diffraction pattern from an α-6T ultrathin film deposited by sublimation.

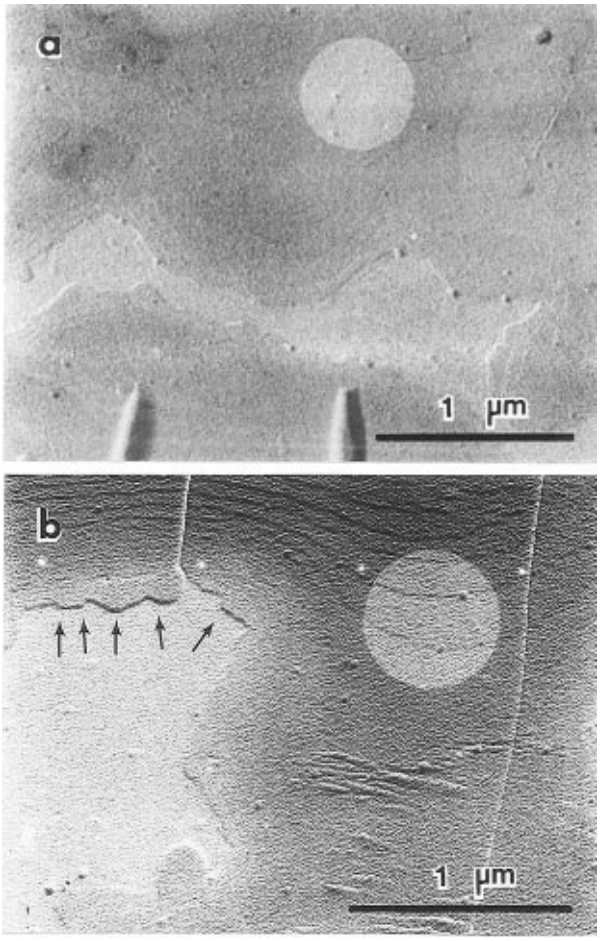

Figure 2. Typical morphologies of α-6T single crystals grown during cooling from the melt in thin films. The brighter circles define areas from which electron-diffraction patterns were recorded. Arrows in b illustrate the level of microfaceting typically seen.

nitrogen and, after evaporation of the solvent, were momentarily heated to 320 °C. Crystals were then grown by cooling from the melt. All treatments were performed under dry nitrogen to avoid degradation. Also, because α-6T sublimes readily, cooling had to be done at a rate of 5 °C/min or greater. As a result, the morphology of our films was not spatially uniform, with polycrystalline regions predominating and with the consequent necessity to explore the electron-microscopic grids in order to find appropriate regions containing large single crystals. In all cases, the films were then shadowed with Pt/C and carbon-coated in a vacuum evaporator prior to being floated off from their mica substrates in water and caught onto electron-microscope grids for examination at 100 kV in a JEOL transmission electron microscope.

Results and Discussion

Crystallization of α-hexathienyl in ultrathin films by sublimation yielded morphologies such as those seen in Figure 1a. The crystals are very small (≤100 nm) and have no regular crystallographic boundaries. These are to be compared to the corresponding morphologies in thicker films of α-6T grown on various substrates for actual device applications (Figures 2 and 3 of ref 17), which were also polycrystalline, but with a high proportion of lamellae in edge-on and oblique orientations. Here, all the crystals appear to have grown flat-on and therefore provide evidence for the mode of vapor deposition of the first molecules onto the substrate and the orientation of the crystalline layer in actual content with the substrate. The fact that the substrate used in this case is amorphous eliminates any possible interfacial influences of a crystallographic or epitaxial nature. Electron-diffraction patterns from crystals such as those of Figure 1a are seen in Figure 1b. Of course, the overwhelming majority of the patterns consists of spotty full circles since the crystals are so small, but we have been successful in some cases (such as Figure 1b) to obtain patterns from a few adjacent crystals that have similar orientations. These are seen to display single-crystal characteristics with a rectangular symmetry. The major interplanar spacings are identified in Figure 1b and correspond to the strongest reflections seen in X-ray diffractograms from bulk specimens of this semiconductor.[17] These spacings arise from the side-by-side packing of chains and imply therefore that the molecules in the original crystals contacting the substrate are oriented close to normal to it.

Much larger crystals are obtained by crystallization from the melt: two typical cases are seen in Figure 2. The crystals are seen to be lamellar and very thin (<10 nm from shadow lengths), implying only a few constituent molecular layers. However, in lateral dimensions they can be very large (typically a few micrometers) and are always accompanied by profuse overgrowths and terraces. A clear characteristic of these crystals of α-6T is their lack of regular crystallographic faceting. This may very likely be a consequence of the relatively rapid cooling that was necessary in order to avoid desorption from the substrate at high crystallization temperatures. There are some indications of geometric microfaceting in Figure 2b (arrowed), from which we infer that this may indeed be the cause.

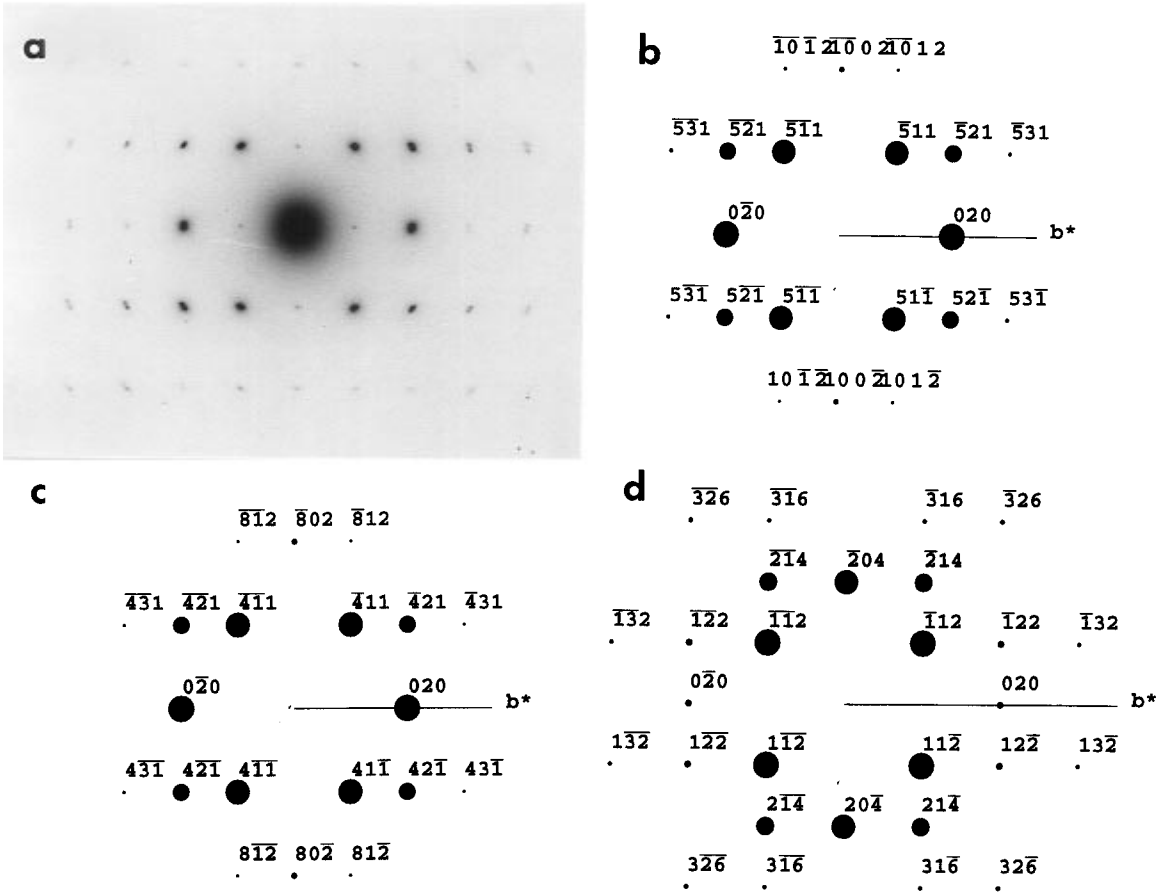

Figure 3. (a) Selected-area electron-diffraction pattern from melt-grown single crystals of α-6T. The reflections are indexed in b−d on the basis of three different published unit cells, i.e., (b) ref 13, (c) ref 14, and (d) ref 15; the latter pattern is rotated 90° relative to the others because of the different axial assignments in this cell.

Typical selected-area electron-diffraction patterns from regions such as those circumscribed within the crystals of Figure 2a,b are as in Figure 3. These very regular single-crystal patterns are entirely consistent with the much spottier ones from vapor-deposited α-6T (Figure 1b). The many orders of reflections seen in both directions are indicative of the high crystallographic order existing in these crystals, and the rectangular projected symmetry shows that the unique monoclinic unit cell axis *b* lies in the plane. Calculated diffraction patterns from three possible unit cells[13−15] are also depicted in this figure in corresponding projections and the reflections identified. The four different unit cells proposed for α-6T[12−15] are shown in Figure 4 in *b*-axis projection; Cell (a) is not considered further, since all later studies[13−15] have shown that the molecules are actually inclined with respect to the cell axes. As seen in Figure 3, the calculated patterns from cells b and c are essentially identical in terms of lattice spacings; the only difference is in the zone-axis and Miller-index assignments. Despite the great similarity in spacings among the cells, we can differentiate between the low- and high-temperature forms (i.e., cells c and d of Figure 4) through their reciprocal-lattice axial ratios, which are 1.458 and 1.283, respectively. The measured axial ratio in our experimental pattern of Figure 3a is 1.420, from which we identify these crystals as corresponding to the low-temperature form.

The orientation of our melt-grown crystals was predominantly as described above throughout our samples. However, by translating our specimens in the electron microscope while observing their selected-area diffraction patterns, we occasionally obtained patterns that

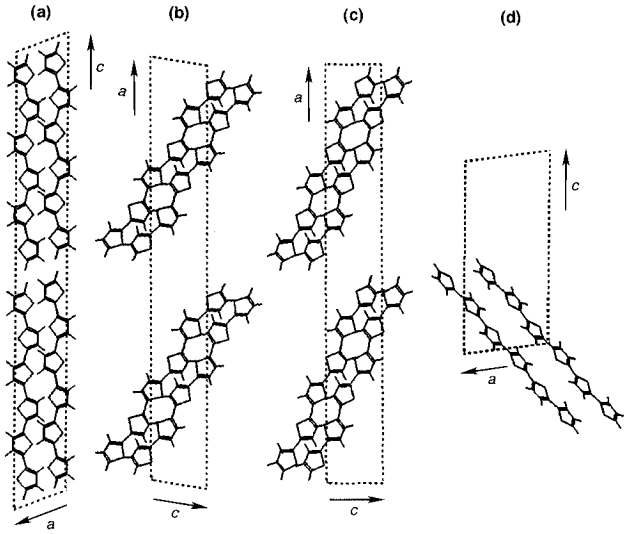

Figure 4. Projections of the four published unit cells for α-6T along their unique monoclinic axis, *b*: (a) ref 12, (b) ref 13, (c) ref 14, (d) ref 15.

were very different from those presented so far. From calculations of their interplanar spacings we believe that these do not represent different polymorphic forms but rather different fortuitous orientations of the crystals on the substrate, which thus allow us to probe the full three-dimensional structure of α-6T. A very interesting and rare case is seen in Figure 5. Here, the horizontal direction contains a long series of closely spaced sharp reflections that we believe arise from the end-to-end packing of the chains. We identify these as *h*00 in terms

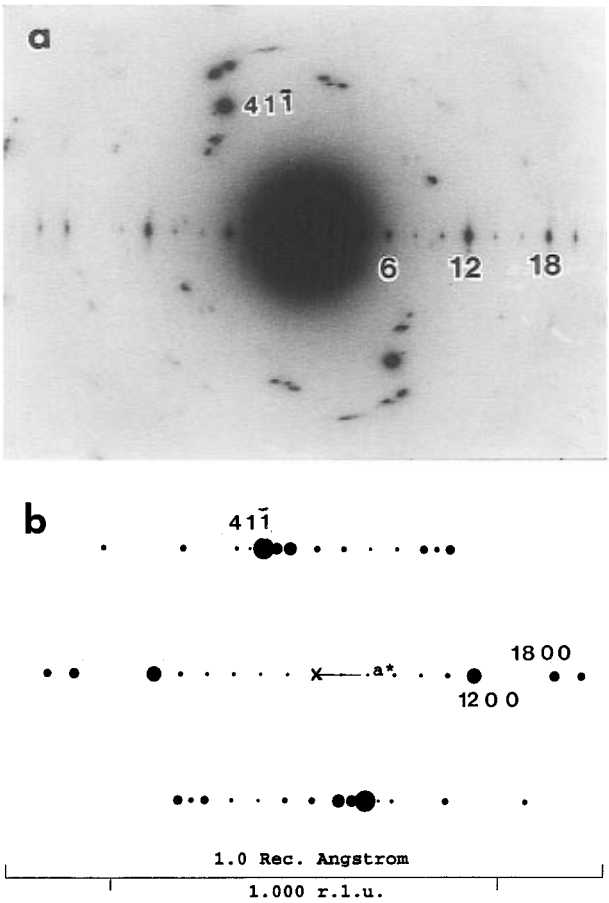

Figure 5. (a) Electron-diffraction pattern of an α-6T crystal showing a full series of chain end-to-end packing reflections (*h*00). (b) Calculated diffraction pattern using zone [011] of the unit cell of ref 14.

of cell c, which, based upon our results above, is the most likely one for our growth conditions (the accompanying calculated diffraction pattern originates from the [011] zone). In those terms, the chain-axis reflections of Figure 5 extend all the way to 20,0,0 (and beyond 30,0,0 in the original negative). The intensities are observed to follow a pattern that maximizes every third reflection up to 18,0,0 (i.e., for $h = 6$, 12, and 18) and the strongest of these is 12,0,0. These data confirm directly the all-trans hexameric structure of this molecule, for which (in a two-chain unit cell) we would predict that the strongest of this molecule, for which (in a two-chain unit cell) we would predict that the strongest reflection (12,0,0) should arise from the *monomeric repeat*. Beyond 18,0,0 the cyclical maximization of intensity for every third reflection breaks down (see, e.g., the 20,0,0 spot in Figure 5). We associate this with the fine-scale structure *within* each monomeric unit, in which the individual sulfur atoms play a dominant role).

It should be noted in Figure 5 that the actual molecular repeat (i.e., the 200 reflection) is not detectable because it is subsumed by the direct beam. However, in a few cases we have been able to preserve this using low-dose and short-exposure techniques. Such a case is shown in Figure 6, where we have highly magnified the central-beam region: Diffracted beams at 2.38 nm are clearly resolved right next to the much stronger transmitted beam; resolution of such large spacings is not usual in electron diffraction, particularly of beam-sensitive materials. The spacings identified in this figure are confirmed by self-calibration from coexisting polycrystalline regions which give rise to the faint

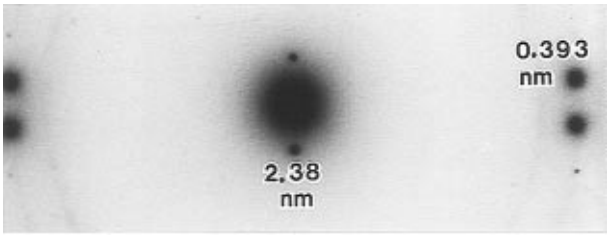

Figure 6. Electron-diffraction pattern demonstrating resolution of the primary molecular repeat at ca. 2.38 nm adjacent to the transmitted electron beam.

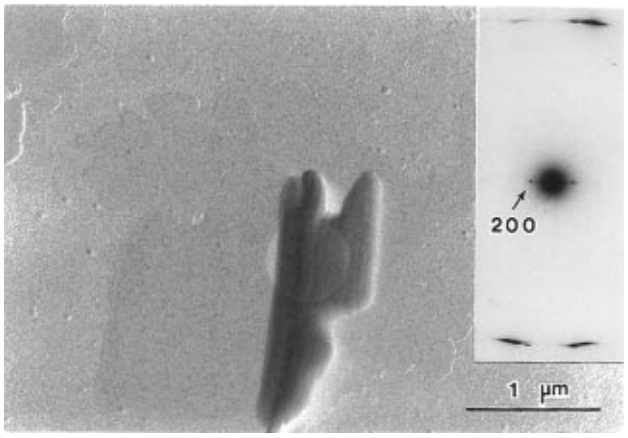

Figure 7. Growth of tall edge-on lamellae seen in a quasi-epitaxial relationship with an underlying flat-on crystal of α-6T; the electron-diffraction pattern from the circled area is seen in correct orientation to the field.

full arcs superimposed at 0.458 and 0.393 nm. The 2.38 nm molecular repeat is slightly larger than that determined from X-ray measurements,[12−14,17] but expansion of the lattice of beam-sensitive organic and polymeric materials under electron irradiation is well-known.[19−21] This direct confirmation of the all-trans conformation of α-6T helps us to recall once again the close analogy with the macromolecular analogue, polythiophene, whose structure is also trans-planar.[22] In this sense, this conjugated hexamer offers a closely appropriate model relating to the π-stacking mechanism of transport in polythiophene.

Diffraction patterns of this kind provide evidence that crystals can also be grown *on edge*, i.e., with their molecules parallel to the substrate. Such cases are rare, but one is seen in Figure 7, where a stack of very tall lamellar crystals is observed to have grown on top of the usual flat-on crystals. It is possible that this might occur through some homoepitaxial relationship, because we found that the two types of crystals generally share a common *b*-axial growth direction. The electron-diffraction pattern (inset in correct orientation to the field in Figure 7) shows that the molecules are oriented close to perpendicular to the lamellae.

As crystals grow in progressively thicker films, additional morphological features of great importance are revealed (see Figure 8a). These include extensive crystallographic fractures that are transverse to the preferred growth direction (i.e., to the *b*-axis, using once again cell c). Moreover, the crystal is seen to splay repeatedly about that axis, leading to the tall ridges parallel to the growth direction. It is interesting to note from the opposite shadowing contrast in the left and right sides of this micrograph that splaying occurs in both directions upward from the central zone. The corresponding diffraction pattern of Figure 8b docu-

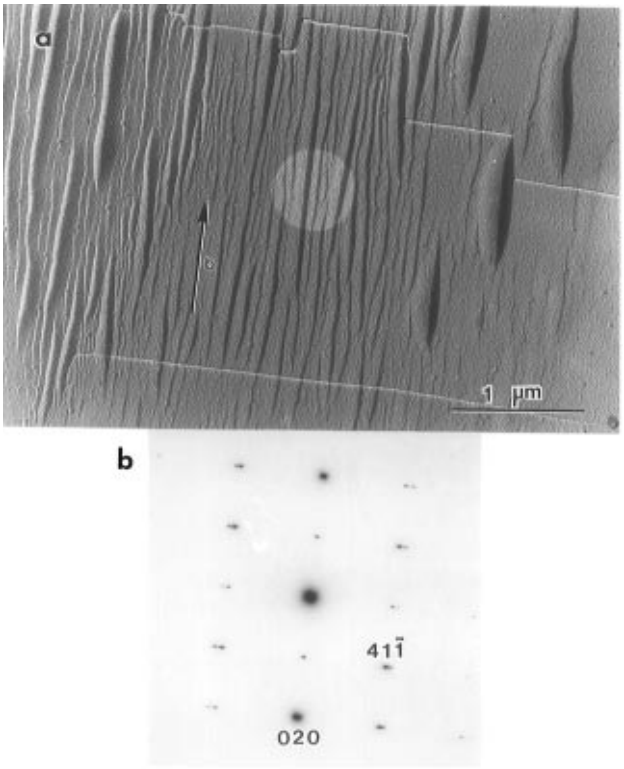

Figure 8. (a) Growth of α-6T from the melt in thicker films, exhibiting transverse crystallographic fractures normal to the growth direction (arrowed), as well as lamellar splaying parallel to it. (b) Electron-diffraction pattern from the circled area in a.

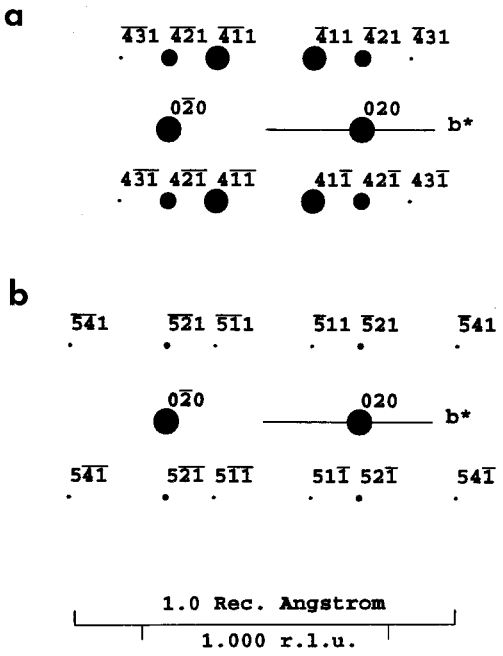

Figure 9. Calculated electron-diffraction patterns for α-6T single crystals along the (a) [104] and (b) [105] zones.

ments this, as well, in the form of the streaked 4*k*1 reflections. We should notice that these are streaked perpendicular to the *b*-axis and that the 0*k*0 reflections themselves are not streaked. The streaking results simply from the elevation of the 5*k*1 peaks into the reflecting position by the splayed crystal ends. As seen in Figure 9, these 5*k*1 peaks are also reasonably intense and are located just outside their 4*k*1 counterparts in reciprocal space. The sharp fracture planes in Figure 8 are seen to cut through most of the splayed lamellae

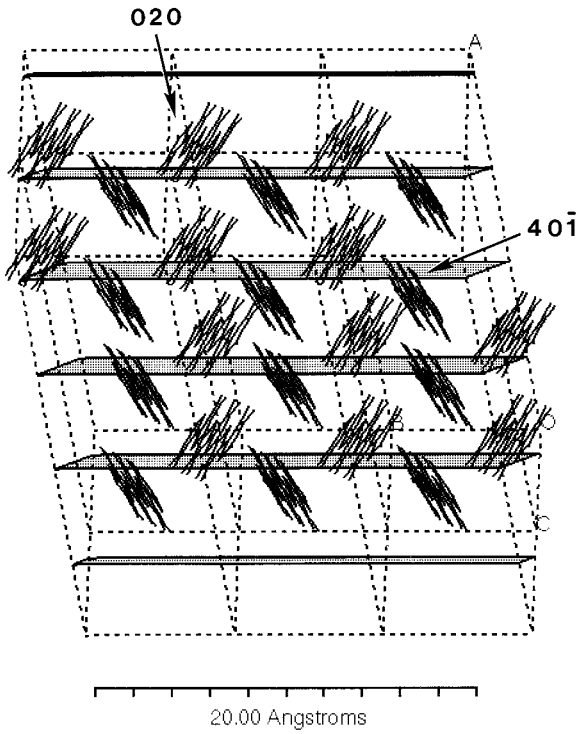

Figure 10. Projection of α-6T molecules close to parallel to their molecular axes, showing their relative dispositions to a substrate (viewed from the top) as well as the origin of the internal fractures. Because of poorer interdigitation, the (020) are seen to be much more facile internal cleavage planes than the equally populated but much better interdigitated (4,0,−1) ones.

and to be interrupted only by the tallest ones. The (020) are indeed very natural crystallographic cleavage planes for α-6T because they contain the molecular chains, whose trans-planar conformation is only slightly inclined to these planes and has poor interdigitation (see Figure 10). On the other hand, the (4,0,−1) planes, which are normal to the (020), also contain the same molecules but in a much better interdigitated manner (see again Figure 10). This explains why cleavage occurs so readily in the first case and rarely in the second. This inherent crystallographic tendency of α-6T toward transverse fracture has severe negative implications toward device fabrication based upon large single crystals, since it is expected that any such crystals will likely contain profuse internal fractures. We have already documented this on samples prepared by rapid high-temperature treatment on various substrates including source and drain pads in a transistor configuration.[23] The field-effect mobility in α-6T thin-film transistors (TFTs) subjected to rapid thermal processing remained constant as the average grain size increased from ca. 100 nm to ca. 1−2 μm. When the crystal size was increased beyond a few micrometers, electrical conductivity through the active film (over a distance in the range of 4−12 μm) was lost. This is presumably a consequence of the internal fractures documented above.

Progressing further in the direction of thicker films, we eventually arrive at three-dimensional (bulk) specimens, whose morphology now begins to approach that of typical organic and polymeric materials solidifying from viscous environments.[24,25] The surface morphology of such a thick sample is seen in Figure 11 using scanning electron microscopy. Mostly the sides of lamellar crystals are visible in Figure 11a, while the growth tips have been imaged in Figure 11b. The

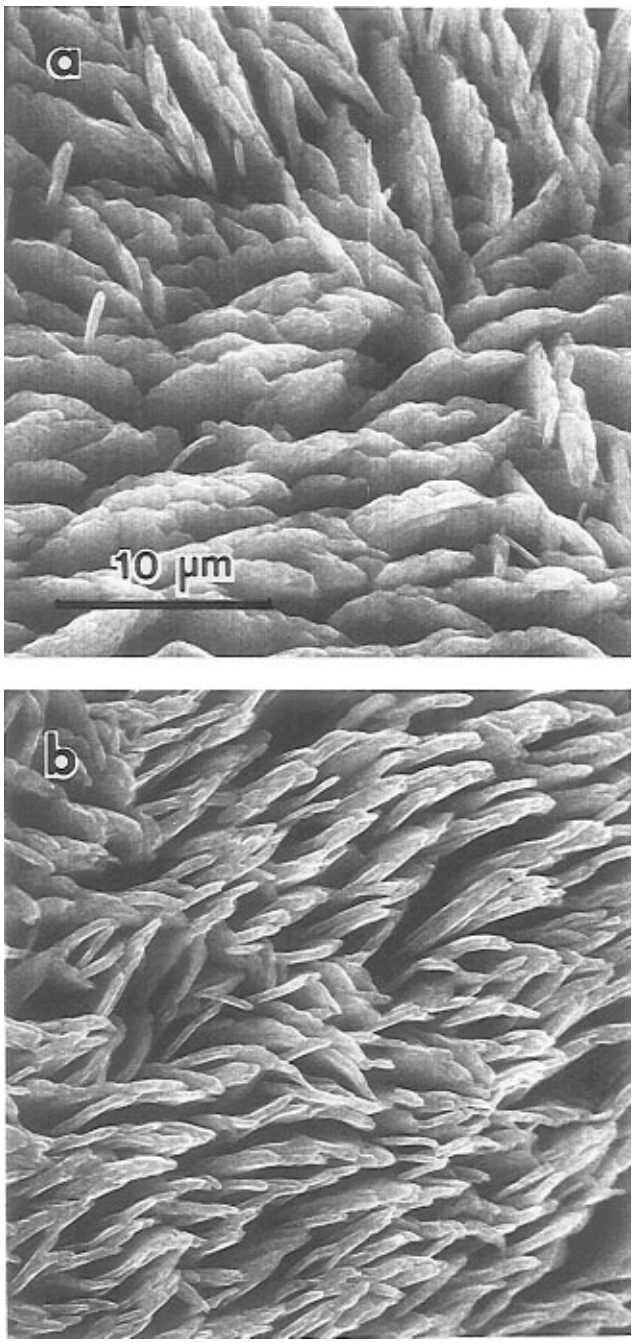

Figure 11. Scanning electron micrographs (secondary electrons) of α-6T bulk-specimen free surfaces, showing structure and packing of lamellar stacks (a) along their sides and (b) at their growth tips.

morphology is now essentially three-dimensionally averaged but retains the major features seen in ultrathin films. The constituent crystals remain lamellar and are now organized in distinct quasi-parallel stacks (for space-filling reasons). No crystallographic boundaries are seen in either the side view or the growth tips.

Conclusions

Over a range of crystallization conditions, α-6T is found to grow in the form of thin, large lamellar crystals with preferred growth along the *b*-axis of the unit cell and with molecular chains normal to the lamellar surfaces. Among the various such cells proposed, we could show through single-crystal growth and precise measurement of appropriate reciprocal-lattice axial ratios that cell c (ref 14) best describes the molecular structure of this material under the conditions grown, which favor the low-temperature form. In previous studies[15,16] we have described conditions and morphologies related to growth of the high-temperature polymorph. A major characteristic of α-6T lamellae is their spontaneous fracture along (020) planes. This is a result of little interdigitation among the α-6T chains which are contained in these planes and which are aligned closely to them. In thicker films the lamellae splay and warp about their growth axes. Both of these characteristics have negative implications for use of this material in potential single-crystal thin-film transistor devices since they introduce lattice discontinuities, deformations, and noncrystalline boundaries. These results should provide a basis for further examination of the transport mechanism in these oligothiophenes in relation to recent low-temperature studies that provide evidence for intrinsic transport.[26]

Acknowledgment. We are grateful to Dr. R. A. Laudise for helpful discussions.

References and Notes

(1) Tsumura, A.; Koezuka, H.; Ando, T. *Synth. Met.* **1988**, *25*, 11.
(2) Koezuka, H.; Tsumura, A.; Fuchigami, H.; Kuramoto, K. *Appl. Phys. Lett.* **1993**, *62*, 1794.
(3) Holland, E. R.; Bloor, D.; Monkman, A. P.; Brown, A.; DeLeeuw, D.; Bouman, M. M.; Meijer, E. W. *J. Appl. Phys.* **1994**, *75*, 7954.
(4) Murase, I.; Ohnishi, T.; Noguchi, T.; Hirooka, M. *Polym. Commun.* **1987**, *28*, 229.
(5) Fuchigami, H.; Tsumura, A.; Koezuka, H. *Appl. Phys. Lett.* **1993**, *63*, 1372.
(6) Fichou, D.; Horowitz, G.; Nishikitani, Y.; Garnier, F. *Synth. Met.* **1989**, *28*, C723.
(7) Horowitz, G.; Fichou, D.; Garnier, F. *Solid State Commun.* **1989**, *70*, 385.
(8) Garnier, F.; Horowitz, G.; Peng, X. Z.; Fichou, D. *Synth. Met.* **1991**, *45*, 163.
(9) Dodabalapur, A.; Torsi, L.; Katz, H. E. *Science* **1995**, *268*, 270.
(10) Katz, H. E.; Torsi, L.; Dodabalapur, A. *Chem. Mater.* **1995**, *7*, 2235.
(11) Lovinger, A. J.; Rothberg, L. J. *J. Mater. Res.* (in press).
(12) Servet, B.; Ries, S.; Trotel, M.; Alnot, P.; Horowitz, G.; Garnier, F. *Adv. Mater.* **1993**, *5*, 461.
(13) Porzio, W.; Destri, S.; Mascherpa, M.; Brückner, S. *Acta Polym.* **1993**, *44*, 266.
(14) Horowitz, G.; Bachet, B.; Yassar, A.; Lang, P.; Demanze, F.; Fave, J.-L.; Garnier, F. *Chem. Mater.* **1995**, *7*, 1337.
(15) Siegrist, T.; Fleming, R. M.; Haddon, R.; Laudise, R. A.; Lovinger, A. J.; Katz, H. E.; Bridenbaugh, P.; Davis, D. D. *J. Mater. Res.* **1995**, *10*, 2170.
(16) Laudise, R. A.; Bridenbaugh, P. M.; Siegrist, T.; Fleming, R. M.; Katz, H. E.; Lovinger, A. J. *J. Cryst. Growth* **1995**, *152*, 241.
(17) Lovinger, A. J.; Davis, D. D.; Ruel, R.; Torsi, L.; Dodabalapur, A.; Katz, H. E. *J. Mater. Res.* **1995**, *10*, 2958.
(18) Katz, H. E.; Dodabalapur, A.; Torsi, L.; Lovinger, A. J.; Ruel, R. *Am. Chem. Soc., Polym. Mater. Sci. Eng.* **1995**, *72*, 467.
(19) Grubb, D. T. *J. Mater. Sci.* **1974**, *9*, 1715.
(20) Keller, A. In *Developments in Crystalline Polymers-1*; Bassett, D. C., Ed.; Applied Science: London, 1982; Chapter 2.
(21) Lovinger, A. J. In *Radiation Effects on Polymers*; Clough, R. L., Shalaby, S. W., Eds.; ACS Symposium Series 475; American Chemical Society: Washington, DC, 1991; Chapter 6.
(22) Brückner, S.; Porzio, W. *Makromol. Chem.* **1988**, *189*, 961.
(23) Torsi, L.; Dodabalapur, A.; Lovinger, A. J.; Katz, H. E.; Ruel, R.; Davis, D. D.; Baldwin, K. W. *Chem. Mater.* **1996**, *7*, 2247.
(24) Keith, H. D.; Padden, F. J., Jr. *J. Appl. Phys.* **1963**, *34*, 2409; **1965**, *35*, 1270, 1286.
(25) Wunderlich, B. *Macromolecular Physics*; Academic Press: New York, 1973; Vols. 1 and 2.
(26) Torsi, L.; Dodabalapur, A., unpublished results.

MA960111B